

NOAA Technical Memorandum NESDIS 10

DETECTION OF HIGH LEVEL TURBULENCE USING
SATELLITE IMAGERY AND UPPER AIR DATA

Gary P. Ellrod

Satellite Applications Laboratory
Washington, D.C.

April 1985

UNITED STATES
DEPARTMENT OF COMMERCE
Malcolm Baldrige, Secretary

National Oceanic and
Atmospheric Administration
Anthony J. Calio
Deputy Administrator

National Environmental Satellite,
Data, and Information Service
John H. McElroy,
Assistant Administrator



TABLE OF CONTENTS

ABSTRACT.....	1
1. INTRODUCTION.....	1
2. SUMMARY OF SATELLITE TURBULENCE SIGNATURES.....	2
3. A CHRONOLOGICAL SEQUENCE OF TURBULENT CLOUD PATTERNS.....	12
4. RELATIVE FREQUENCY OF TURBULENCE SIGNATURES.....	14
5. PREVAILING ALTITUDES.....	16
6. DISTINGUISHING TURBULENT FROM NON-TURBULENT FEATURES.....	18
7. CONCLUDING REMARKS.....	28
ACKNOWLEDGEMENTS.....	28
REFERENCES.....	29

DETECTION OF HIGH LEVEL TURBULENCE USING SATELLITE IMAGERY AND UPPER AIR DATA

Gary Ellrod
Satellite Applications Laboratory (NESDIS/NOAA)
Washington, D.C.

ABSTRACT

The primary cloud patterns observed in satellite imagery which relate to high altitude non-convective turbulence are described. Relative frequencies, prevailing altitudes and intensities of each type are presented. Means of distinguishing turbulent from non-turbulent cloud signatures based on both satellite imagery and upper wind data are also provided.

1. INTRODUCTION

One of the major problems of the aviation forecaster is detecting and predicting the movement of areas of high level, non-convective turbulence. This traditionally refers to turbulence above 18,000 feet, including clear air turbulence (CAT) and mountain waves. For the continental U.S., short range forecast advisories known as SIGMETS are now issued by the National Weather Service (NWS) National Aviation Weather Advisory Unit (NAWAU) in Kansas City for moderate or greater turbulence as well as thunderstorms, icing and significant areas of reduced ceilings and visibilities. Longer range forecasts of turbulence (out to 12 hours) for much of North America, the North Atlantic and North Pacific Oceans are provided by the National Meteorological Center (NMC) and appear on its significant weather forecast maps. Forecasts out to 24 hours for the continental U.S. are also disseminated in alphanumeric form from Kansas City in aviation Area Forecasts (FAs).

Early research on high level turbulence was based primarily on wind and temperature data from aircraft and radiosonde reports. From these studies (e.g., Endlich, 1964; Rammer, 1973; Sorenson and Beckwith, 1975), it has been determined that turbulence is more likely with curving jet stream segments, mainly in conjunction with sharp troughs or ridges. Turbulence is more pronounced during the winter months when the jet stream is strongest. Turbulence has been associated with upper level, sloping baroclinic zones where horizontal temperature gradients are strong, resulting in large vertical and horizontal wind shears.

Radiosonde data has good vertical resolution, but upper air stations are often separated by distances greater than the width of the turbulent area. Additionally, there is a twelve hour time interval between reports, making it difficult to detect rapid changes in conditions which may produce turbulence.

The launch of geostationary satellites in the early 1970's provided a new potential tool for monitoring turbulence-producing weather systems. Half-hourly satellite pictures provided the temporal and horizontal resolution lacking in the radiosonde data. Since then, meteorologists have been attempting to correlate the occurrence of turbulence with cloud patterns or distinctive cloud signatures in the satellite imagery and their associated flow patterns. Some success has been achieved and the findings have been recently summarized by Smigielski (1984) and Gurka (1983).

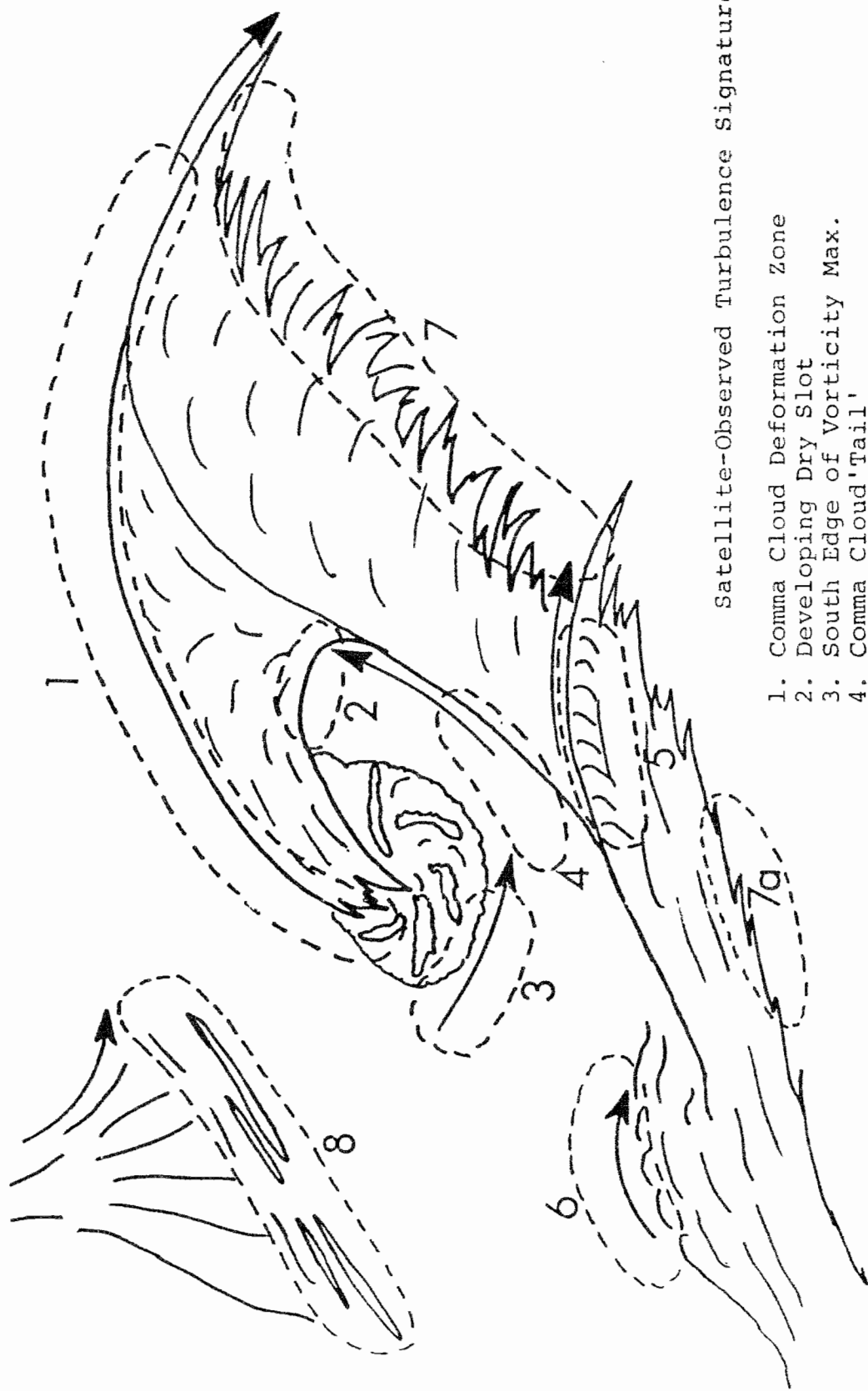
One difficulty to date with these turbulence signatures is that turbulence does not always occur when they are observed. For these features to have better utility in forecasting, more information is needed on the probability of turbulence for each specific cloud signature, and criteria developed to distinguish turbulent from non-turbulent cloud patterns. This report will attempt to provide some of this information through the use of both satellite imagery and horizontal fields of divergence, temperature and vorticity derived from standard pressure level upper wind data. Horizontal analyses are emphasized in this report since it is felt that they best relate to features observed in satellite imagery. This does not negate the importance of vertically derived parameters such as wind shear and Richardson Number.

2. SUMMARY OF SATELLITE TURBULENCE SIGNATURES

Satellite-observed turbulence signatures fall into two main categories: (1) wave clouds usually observable only in high resolution (1 km) visible images and (2) cloud or moisture boundaries observable in all types of imagery, including the 6.7 μm water vapor channel. The following is a brief description of most of the large scale cloud patterns or features observable on infrared (IR) satellite pictures which have been associated with high level turbulence. Not included in this discussion are the smaller scale mountain wave clouds and billow clouds. Mountain waves occur most often at low and middle levels (below 18,000 feet). High level wave clouds not associated with terrain, known as billow clouds, are sometimes seen in conjunction with the large scale features mentioned below. In most cases, billow clouds are an indication of moderate to severe turbulence (Beckman, 1981). They result from a breaking wave phenomenon known as Kelvin-Helmholtz instability which occurs in strong vertical wind shear and high static stability (Ludlam, 1967). The cloud types are shown schematically in Figure 1 along with arrows which represent the typical locations of maximum jet stream winds. The numbers below corresponds to the types indicated in Figure 1.

A. Type 1: Comma Cloud Deformation Zones

Weldon (1979) describes a deformation zone as a region of hyperbolic flow where air parcels undergo stretching along one axis and contraction in the orthogonal direction. For a stationary or slow moving weather system, they relate closely to the cols in the upper flow as depicted by the shaded portions of Figure 2. For a moving system, however, they are not easily identified in the upper wind data. Fortunately, their locations can usually be determined from satellite imagery, regardless of their movement. In infrared and visible images, deformation zones often mark the location of significant cloud boundaries. If not, they can usually be identified by moisture boundaries in the 6.7 μm channel. Turbulence occurs within 2 or 3 degrees latitude (330 km) of the deformation boundary, both in clear air and in cirrus clouds. In this



Satellite-Observed Turbulence Signatures

1. Comma Cloud Deformation Zone
2. Developing Dry Slot
3. South Edge of Vorticity Max.
4. Comma Cloud 'Tail'
5. Transverse Banding
6. Sharp Bulge Along Jet Cirrus
7. Leading Edge of Baroclinic Zone Cirrus
8. Northwest Flow Deformation Zone

Figure 1 A schematic composite showing locations of high level turbulence relative to features commonly observed in IR satellite imagery. Arrows show typical locations of maximum jet stream winds.

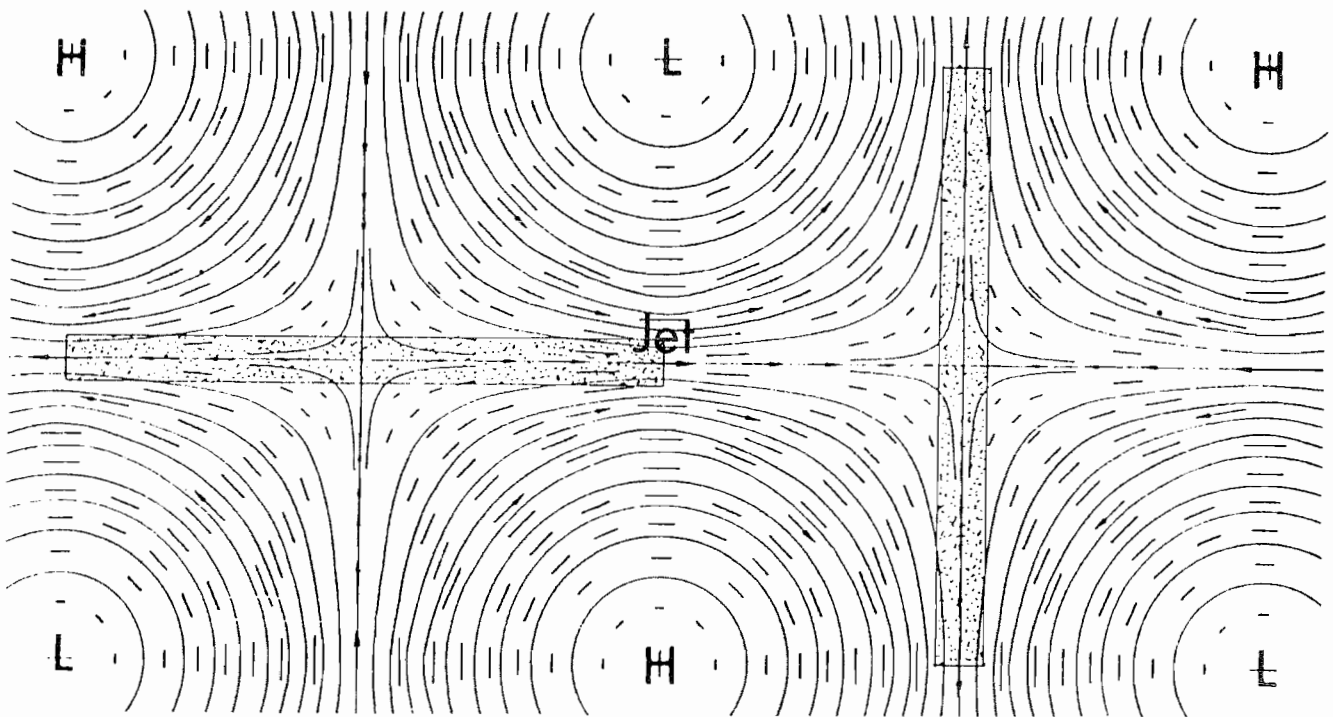
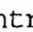
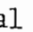


Figure 2 Locations of deformation zones (shaded areas) in a nearly stationary flow pattern. The deformation zone at right (in exit region of jet) is called a "transverse" type, the one at left (in entrance region of jet) is a "longitudinal" type. Short lines are wind vectors, long lines are streamlines or height contours (from Weldon, 1979).



Figure 3 GOES IR image at 1500 GMT April 2, 1984 showing a region of turbulence in a deformation zone along the north edge of a storm comma cloud system over the north central U.S. Symbols  and  represent moderate and severe turbulence, respectively. Winds (kt) are shown for 300mb.

report, cloud pattern type 1 refers to the deformation zone which occurs to the poleward side of a comma cloud associated with a developing cyclone or a vorticity maximum. Northwest flow type deformation zones, which have a different appearance in the imagery, are discussed later.

The most significant turbulence with a comma cloud deformation zone occurs in conjunction with a developing cyclone. Near the "head" of the comma cloud, the most severe turbulence occurs during the formation of a cut-off low and then again when the low is forced to open up by a trough approaching from the west. Along any portion of this deformation zone, turbulence is accentuated when a confluent jet merges with the cloud boundary. An example of a turbulent deformation zone associated with a spring storm is shown in Figure 3. Turbulence is occurring near and east of the upper ridge (maximum anticyclonic curvature) along the deformation zone as it pushes northward.

Mancuso and Endlich (1966) found that deformation is probably the most important large scale kinematic property present in turbulent conditions. Deformation zones are frontogenetic in nature, provided that the winds intersect the isotherms at a large angle (as in Figure 4). Upper level fronts have previously been discussed as an important factor in high level turbulence production (e.g. Endlich, 1964).

B. Type 2: Developing Dry Slots

Turbulence sometimes occurs in the vicinity of the indentation along the back edge of the comma cloud as cyclogenesis progresses (area 2 in Figure 1). This so-called dry slot region occurs directly ahead of a jet maximum which is rotating around the upper trough. The jet will sometimes continue to push through the comma cloud and cross over the ridge line. When this happens, the jet location on satellite photos will often be marked by a sharp boundary between higher cirrus on the anticyclonic side and the lower layers forming the comma head. The dry slot may still be present in the comma head but by this time, high level turbulence has diminished or moved downstream. Figure 5 shows a developing comma cloud system over the southeast U.S. with turbulence located within and preceding the slot.

C. Type 3: Near the Southern Boundary of a Low Cloud Field Associated with the Polar Jet

Although no cirrus is found in these situations, high level turbulence can occur along the southern fringe of a spiraling low or mid cloud field (area 3, Figure 1). This occurs most often with a "digging" or southeastward moving vorticity maximum accompanied by strong cold advection. The cloud boundary marks the approximate location of the Polar jet stream. Figure 6 is an example of this cloud pattern which produced turbulence.

D. Type 4: Along the Back Edge of Jet Cirrus

The western edge of baroclinic zone cirrus along the tail portion of a comma cloud (area 4, Figure 1) is sometimes a location of high level turbulence. The turbulence usually occurs very close to the cloud border. This feature often is associated with a short wave trough just to the west of the jet axis. The confluent upper flow pattern in these cases is usually similar to the "longitudinal type" deformation zone which is found in the entrance region of

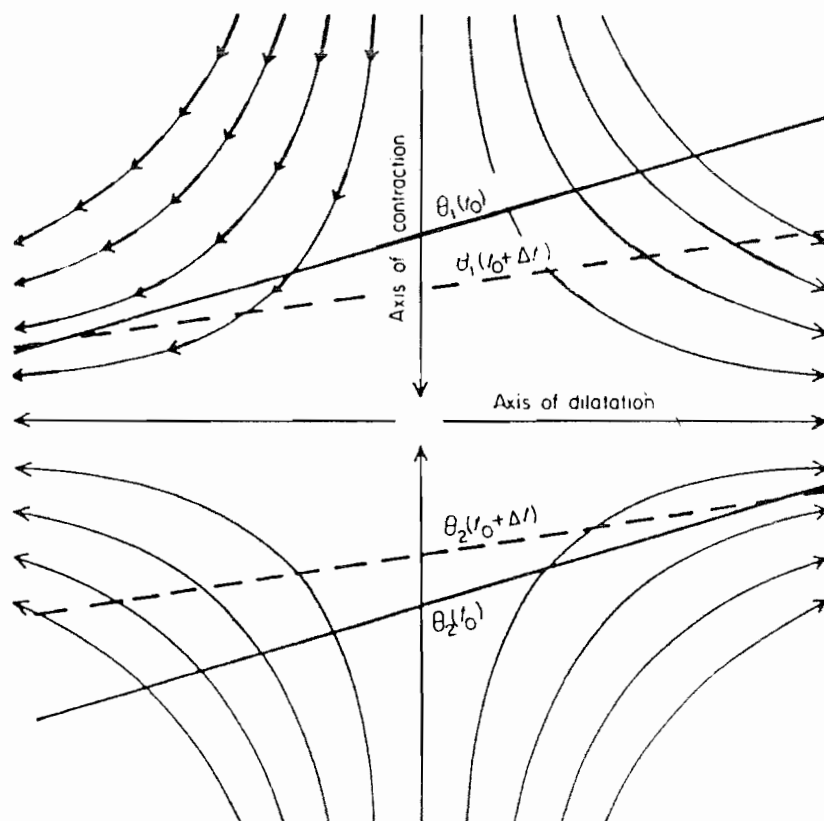


Figure 4 Frontogenesis in the region of a pure deformation zone, with successive positions of two potential temperature isopleths (from Palmén and Newton, 1969). The deformation zone in satellite images is defined by the axis of dilatation.

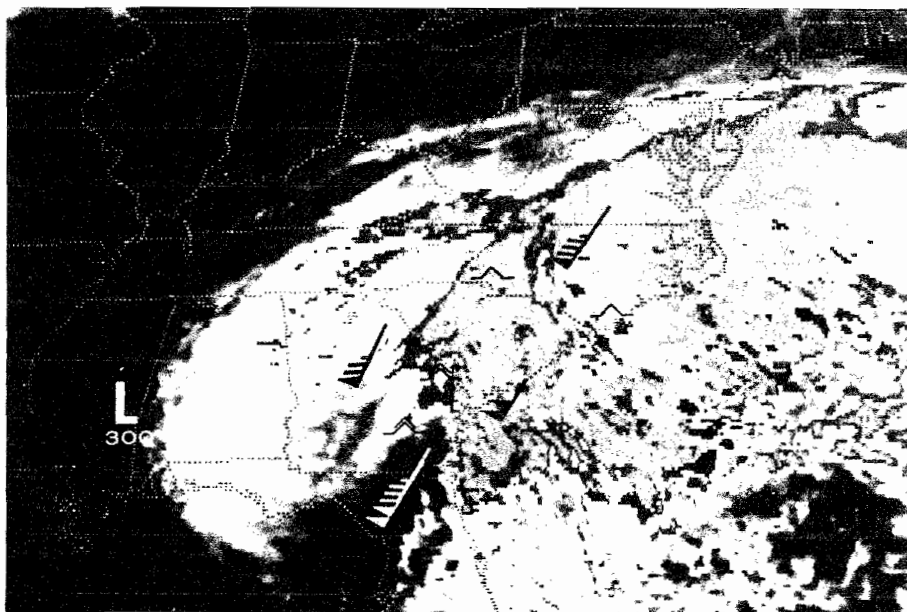


Figure 5 GOES image for 2330Z February 13, 1983 showing turbulence in the region of a developing slot in a comma cloud system. Winds (kt) are shown for 300 mb. Note the rapid deceleration across the cloud boundary.

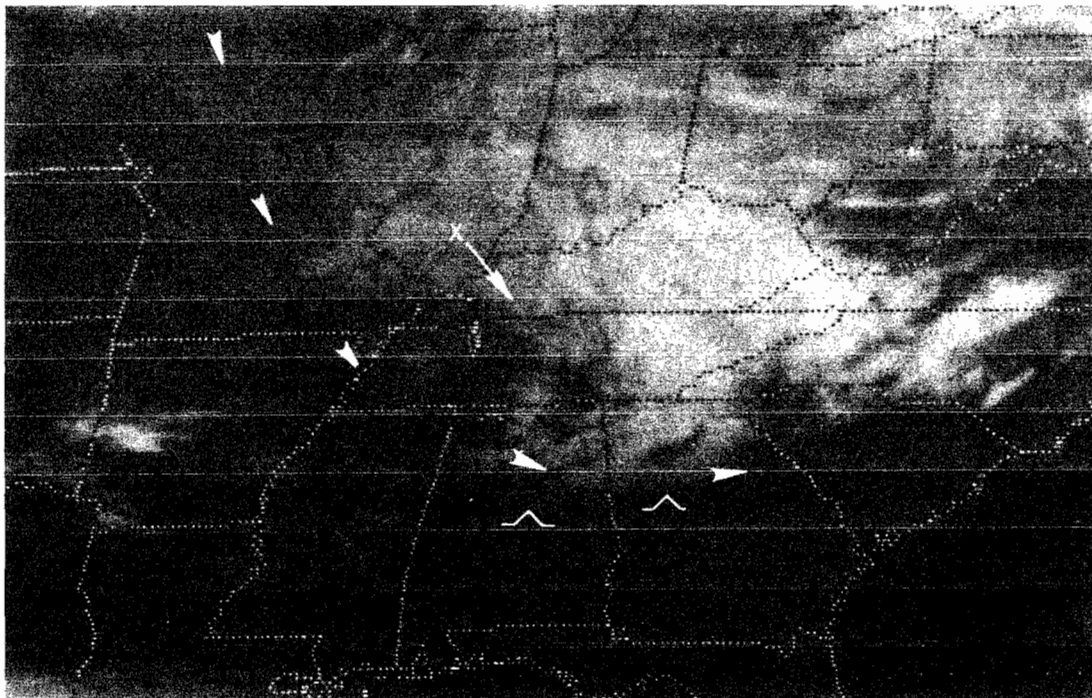


Figure 6 GOES IR image for 2300Z January 11, 1983. Turbulence is occurring in advance of a "digging" vorticity maximum (X). The polar jet at 300 mb is marked by arrowheads.

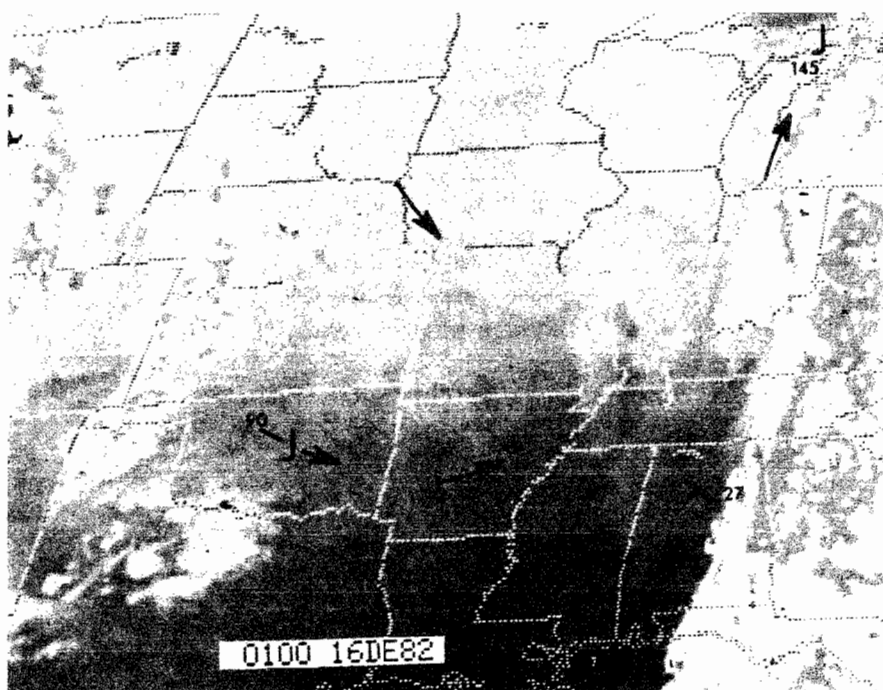


Figure 7 GOES IR image at 0100Z December 16, 1982. Upper flow pattern is shown for 300 mb.

the jet stream (see Figure 2). Figure 7 shows an occurrence of turbulence along this jet boundary and the associated upper flow pattern.

E. Type 5: Transverse Bands on the Anticyclonic Side of the Jet Axis

Wave-like bands in jet stream cirrus whose spacing is more irregular than mountain waves are most often observed on the equatorward side of the subtropical jet stream over the southern United States. The bands are oriented orthogonal to the flow and are often anticyclonically curved. Their presence has been related to strong vertical and horizontal wind shears (Viezee, et al., 1967) in the upper flow. The wavelength of the bands is usually sufficient for detection in infrared images. Severe turbulence is just as likely to occur when the bands are relatively wide and thick, resembling convective plumes. Figure 8 is an example of this type of transverse banding which was associated with strong turbulence. The lapse rate in the turbulent layer was nearly adiabatic, determined from nearby radiosonde data at 00Z. The vertical wind shear was about 5 kt/thousand ft, which is considered moderately strong.

F. Type 6: Sharp Anticyclonically Curved Bulges Along the Poleward Edge of Jet Cirrus

As Figure 1 suggests, sharp anticyclonically curved bulges (hereafter referred to as ACBs) along the jet stream cirrus relate to jet streaks, with the maximum winds located near the crest of the cirrus bulge. When turbulence occurs, wind speeds in the jet are usually 80 kt (40 m sec^{-1}) or greater. The wavelength of these features is short, on the order of 500nm (900km) or less. The edge of the cirrus may have a scalloped or ragged appearance, sometimes with transverse bands or billow clouds embedded. In most cases, the ACBs are stable longitudinal waves along the jet which do not develop into cyclones. The shape of the cloud feature can probably be accounted for by ageostrophic accelerations in the vicinity of jet streaks, shown schematically in Figure 9. The turbulence usually occurs from the crest of the ACB downwind for several hundred kilometers. This is the exit region of the jet where the air parcels decelerate rapidly. Figure 10 is an example of the feature in the imagery.

G. Type 7: The Leading Edge of Baroclinic Zone Cirrus

This feature is marked by many parallel cirrus streamers or bands which are oriented across the direction of upper flow. The turbulence occurs within about 200 km of the ragged leading edge of the clouds. Synoptically, it occurs near the upper ridge line or a negative vorticity axis and as a result, the cirrus usually has sharp anticyclonic curvature. Turbulence is more likely to occur with sharp ridge lines in advance of a strong jet (as shown in the lower portion of Figure 1). At the northern end, the cirrus sometimes tapers into a point or "finger". This is a preferred location for the jet to the east of the upper ridge. I will also include with this type all turbulence along the southern edge of subtropical jet cirrus (area 7a) which often has a similar appearance in the imagery. An example of this feature is shown by Figure 11.

H. Type 8: Northwest Flow Deformation Zones

These differ from the deformation zones identified by area 1 in that they occur in west or northwest flow and usually are not associated with developing surface lows. They also have a different appearance in the imagery since the

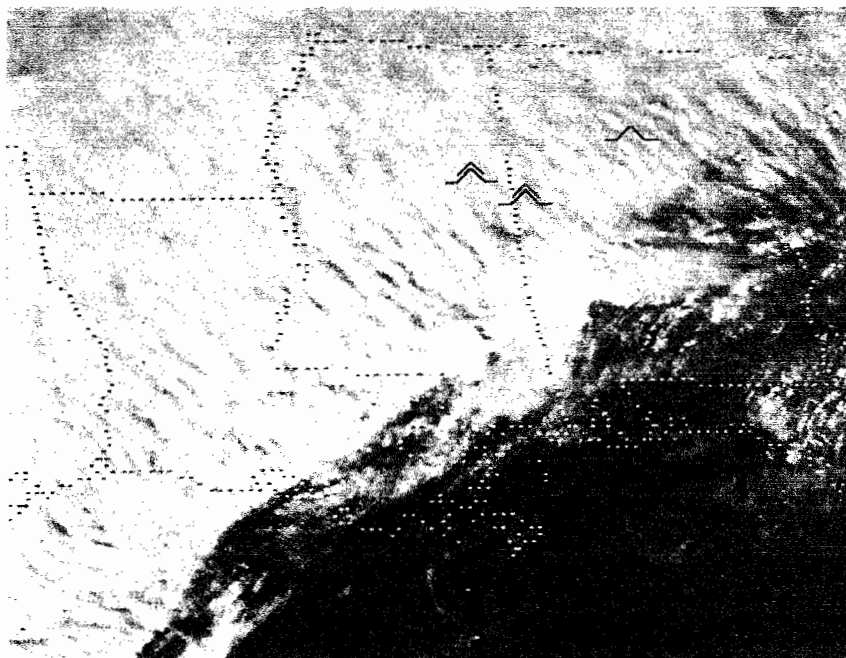


Figure 8 GOES visible image for 2100Z January 31, 1985 showing transverse bands embedded within a multi-layered frontal band. Thunderstorms are developing along the front in southern Alabama.

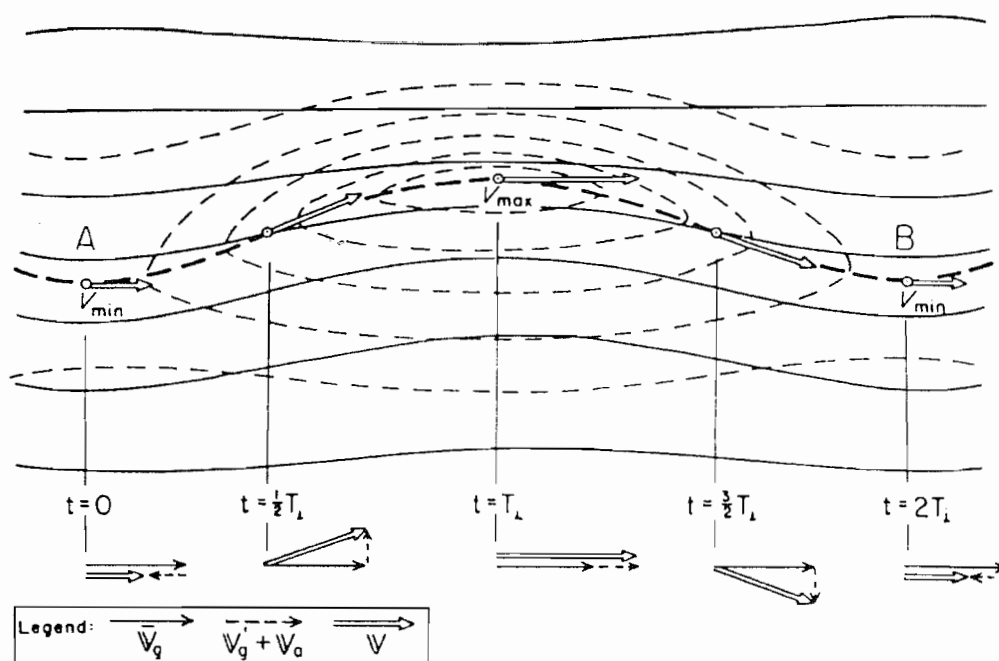


Figure 9 Schematic showing the path of an air parcel in the vicinity of a jet streak. Contours (solid lines), isotachs (thin dashed lines) and vector winds (arrows) are shown (from Palmén and Newton, 1969).

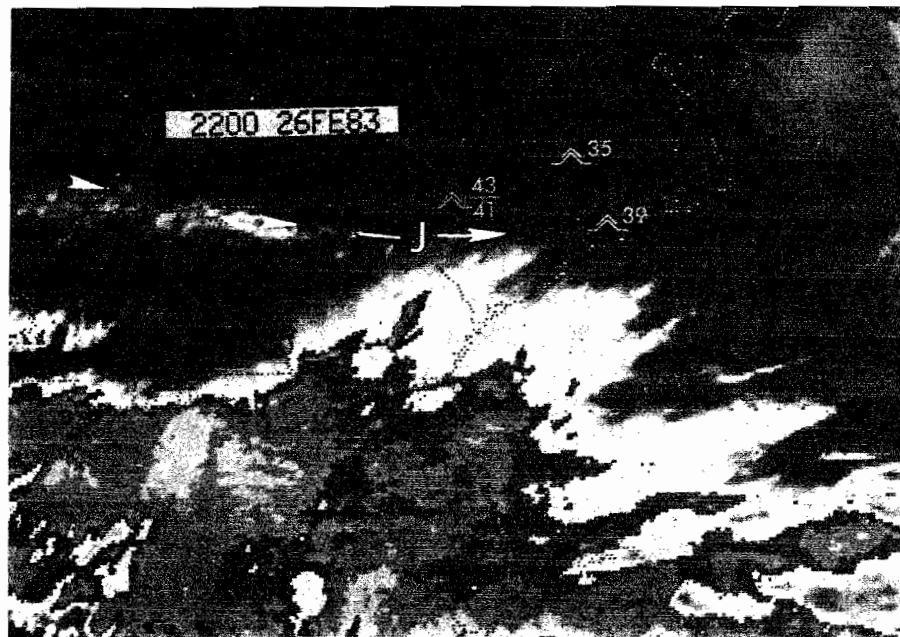


Figure 10 GOES IR image at 2200Z February 26, 1983 showing turbulence with an anticyclonic cirrus bulge along the jet (J).

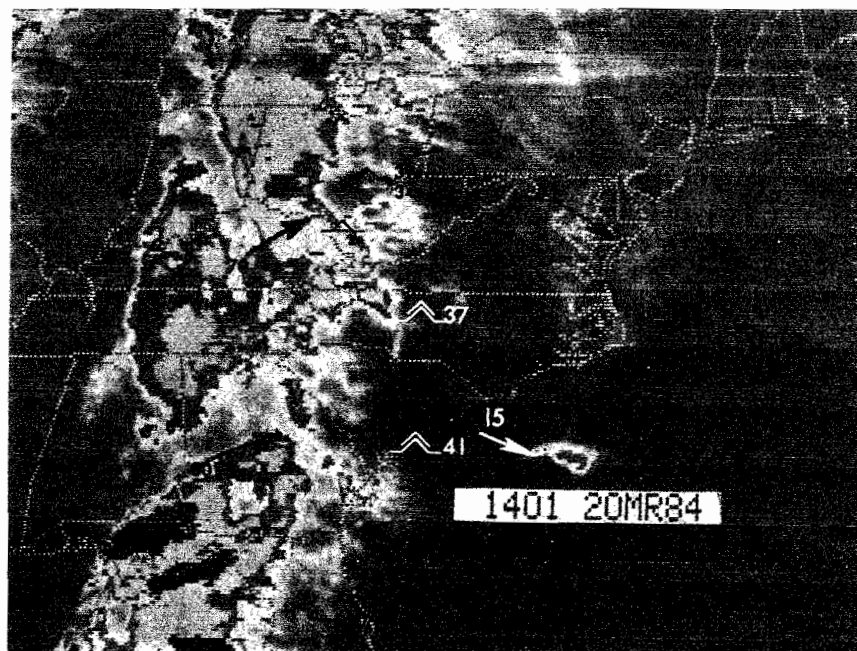


Figure 11 GOES IR image at 1401Z March 20, 1984 with 250 mb wind data. Turbulence is occurring along the leading edge of baroclinic zone cirrus.

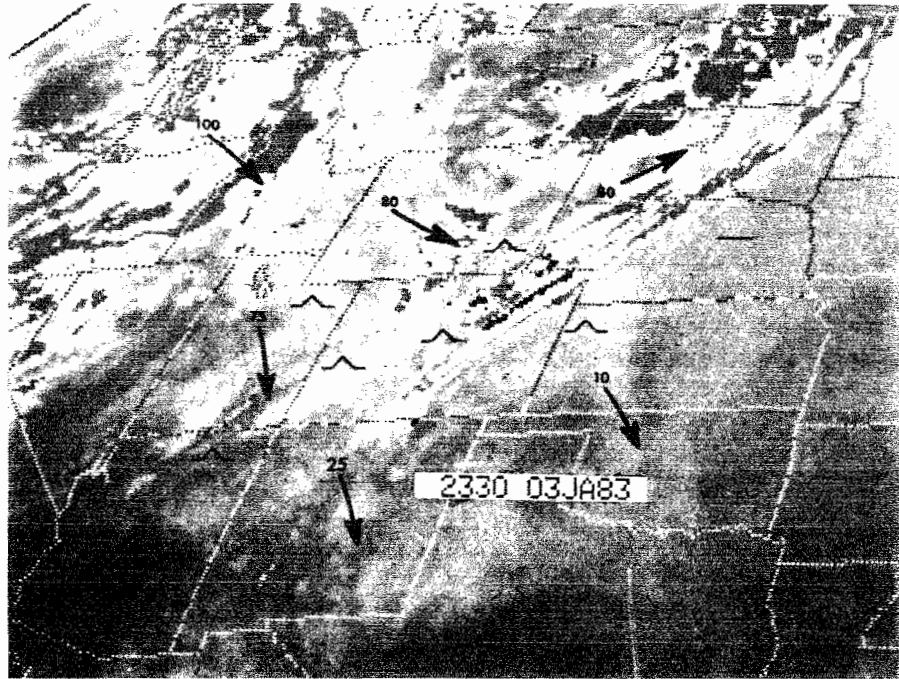


Figure 12 GOES IR image at 2330Z January 3, 1983. Turbulence is occurring with a northwest flow deformation zone.

cirrus often forms in elongated bands transverse to the flow, probably due to the presence of gravity waves. The cirrus can appear as a triangular-shaped area known as a "delta" region. The appearance of this feature varies considerably, depending on the availability of moisture. The turbulence again occurs within 2 or 3 degrees latitude (330 km) of the leading edge of clouds. A maximum in the jet stream winds is located upstream, with the turbulence occurring in the right front quadrant of the jet (Figure 1). Figure 12 shows a typical northwest flow deformation zone over the northern Rockies.

3. A CHRONOLOGICAL SEQUENCE OF TURBULENT CLOUD PATTERNS

Figure 13 is a schematic which shows a possible chronological sequence of typical cloud patterns and related turbulence areas which would occur as a series of jet streaks rotate around a long wave trough and produce cyclogenesis (12a-c). The type of cyclogenesis depicted is one of the most frequent, often referred to as cold air vortex cyclogenesis. The sequence is carried out to the stage when the upper low opens into a trough which is ejected by an approaching upstream shortwave trough (12d-e). The time interval between each schematic varies, but an average of 24 hours may be used for the purpose of this discussion. Some of the turbulent areas may not occur in certain situations, depending on the prevailing upper level conditions which will be discussed in some detail in Section 5.

At time (a), a strong jet maximum is shown plunging down the west side of the upper trough. High level turbulence is occurring with a deformation zone (8) preceding the jet. A comma cloud or baroclinic "leaf" may be present on the poleward side of the jet. East of the trough, an extensive shield of cirrus or multilayered clouds associated with the main baroclinic zone is present.

At time (b), the jet streak has reached the base of the trough and is beginning to turn to the north. The comma cloud begins to expand rapidly as cyclogenesis proceeds. Turbulence breaks out in the deformation zone north of the comma (1) and near the developing dry slot (2) along the back edge of the comma. At this stage, a new jet usually begins to develop near (1). Turbulence may also develop along the leading edge of the baroclinic zone cirrus (7) as stronger winds cross the cloud band toward the upper ridge.

Time (c) shows that the comma has expanded to its maximum size and the dry slot has become well defined. Turbulence areas (1) and (2) have now merged. In situations where the jet does not cross over the comma head (cloud tops in the head are uniformly high and cold) areas (1) and (2) remain separate. At this time, an upper level closed low often forms (at L). If another jet maximum dives into the trough from the northwest, turbulence areas (3) and (4) may become active along the southern fringe of related low cloudiness and the jet cirrus border, respectively.

By time (d), the comma has become sheared out along the upper flow. Turbulence is limited to the region where the jet crosses the base of the comma at (1) (usually near the intersection of the surface occluded front with the cold and warm fronts, known as the triple point). This area is by now well downstream from the upper trough. It is at this stage that turbulence with sharply curved cirrus bulges (6) most often occurs.

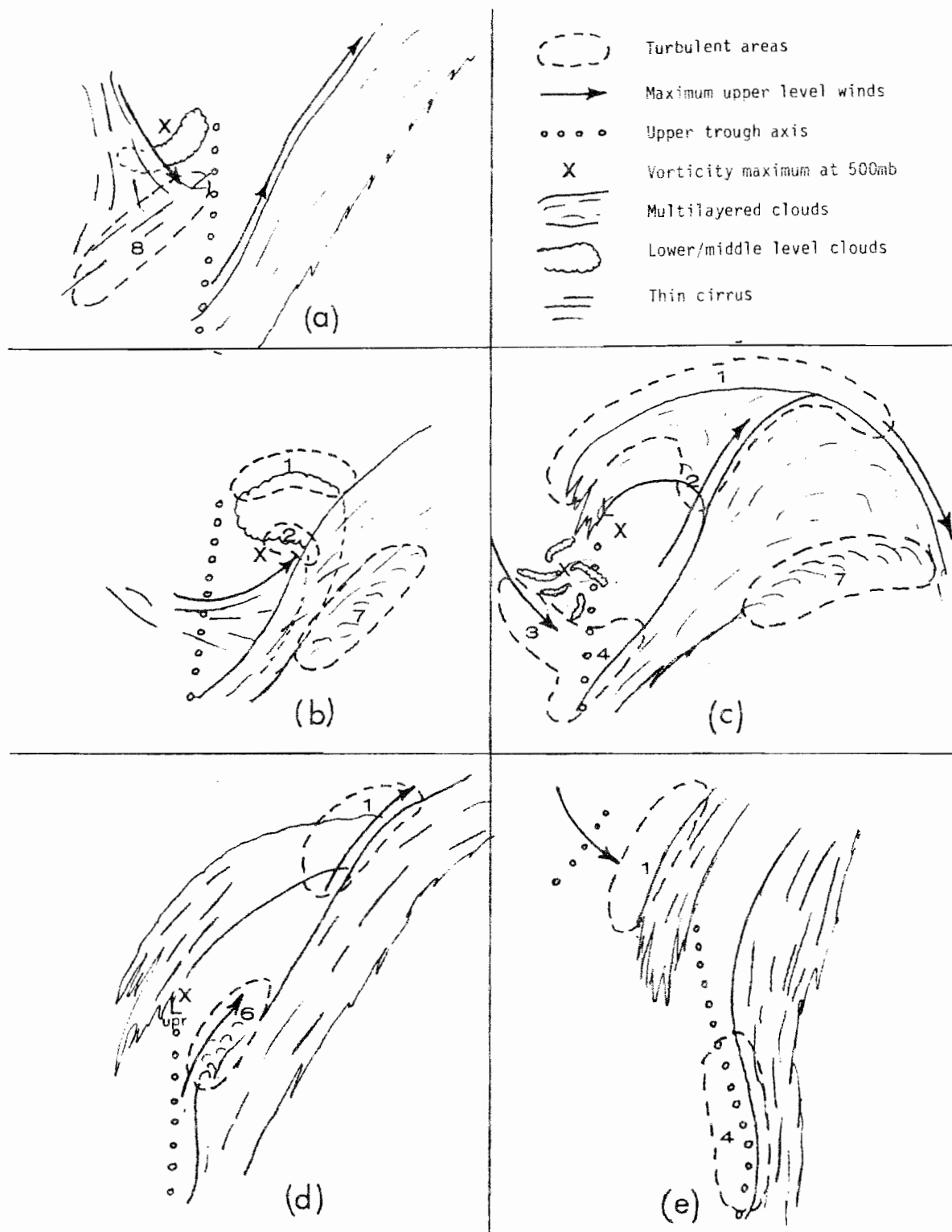


Figure 13 Schematic showing a possible chronological sequence of cloud patterns observed with an evolving storm system, along with regions of high level turbulence.

When a strong upstream shortwave trough approaches the system at time (e), the upper low is forced to "open up" and the primary trough is then ejected to the east or northeast. The area near the old comma head (1) becomes turbulent again. Turbulence may also occur near the back edge of the jet cirrus at (4) as the trough is forced to move rapidly eastward. In fact, the entire cycle which began at time (b) may be reinitiated along the lower portion of the baroclinic cloud band if the trough acquires a negative tilt (northwest to southeast orientation). If the primary trough becomes positively tilted instead (oriented northeast to southwest), the remnants of the comma head dissipate and turbulence occurs along and northwest of the trough. Which of these two scenarios occurs depends on the relative location of the approaching jet maximum. If it slides over the top of the primary trough, a positive tilt is more likely.

4. RELATIVE FREQUENCY OF TURBULENCE SIGNATURES

In an effort to determine which cloud signatures are more likely to produce turbulence, a survey was conducted for a 5-month period over the continental U.S. The total number of turbulence signatures observed in the imagery for each type was determined, along with the percentage of cases of both moderate or greater turbulence and severe turbulence.

Infrared satellite images from GOES East and West were examined for the period from October 1982 through February 1983. The cloud patterns were compared with those commonly found to produce turbulence. The occurrence of turbulence was verified with plotted charts of high altitude pilot reports (pireps) produced by the Aviation Branch of the National Meteorological Center (NMC). These reports are plotted for the period from 0900Z to 0300Z daily, the times of peak aviation traffic. Not included in the survey was a region across the extreme northern U.S., from northern Michigan westward to northern Idaho plus extreme northern New England. This area has significantly fewer pilot reports due to a limited number of commercial jet flights. Also, some weekend days were not included, depending on the density of pireps received.

The data sample was divided into two groups. The first group included signatures occurring over the Rocky Mountains, the second consisted of signatures east of the Rockies. In this way, effects of higher terrain could be estimated. In cases where the cloud patterns overlapped into both regions, they were included in both data sets.

The results are tabulated in Table 1, expressed in percent of observed occurrence for each cloud pattern type. The percentages are probably somewhat low due to the likelihood that turbulence may have occurred in some cases but was not encountered by aircraft or for some reason was not reported. In any case, the numbers should be good indicators of the relative turbulence threat of all the cloud pattern types. About 77% of all turbulence cases could be accounted for by the cloud patterns shown in figure 1.

As expected, the percentages were lower east of the Rockies for all cloud types. The cloud signatures with the highest percentage of turbulence were types 1 (comma cloud deformation zones), 2 (developing dry slots), 6 (ACBs) and 8 (northwest flow deformation zones). Types 2 and 8 however, were

relatively infrequent. The highest threat of severe turbulence occurred with types 1, 2, 5 and 6. The frequencies of severe turbulence ranged from 21 to 31 percent for these types.

One of the forecasting rules used by NMC is that the region north of a developing cyclone nearly always has high level turbulence (Rammer, 1973). There were 20 type 1 deformation zones in this study which were associated with deepening lows. Of this sample, 87% had moderate or greater turbulence while about 50% had severe turbulence. However, these were only a small portion of all the type 1 deformation zones observed.

Table 1
Relative Frequency of Turbulence-Producing Satellite Cloud Patterns
(Expressed in Percent)

Signature Type	East of Rockies (%)		Over Rockies (%)		Entire (%) U.S.		Total Number of Cases
	MOGR	Severe	MOGR	Severe	MOGR	Severe	
1	64	24	71	32	67	27	161
2	69	31	80	13	75	21	28
3	37	9	58	11	44	9	54
4	55	16	82	16	65	16	113
5	42	22	55	0	50	16	62
6	72	21	83	33	75	25	59
7	56	8	72	16	58	11	108
8	78	11	50	50	73	18	11

In the overall totals, the most threatening cloud signatures with respect to both occurrence of moderate or greater and severe turbulence were: (1) large scale deformation zones (both northwest flow and comma cloud types), (2) ACBs and (3) developing dry slots associated with cyclogenetic comma clouds. Transverse-banded cirrus produced severe turbulence a relatively high percentage of time east of the Rockies but did not fare as well in the overall totals. Since this banding has long been recognized as a source of high level turbulence, it is possible that aircraft avoid these regions deliberately, thus reducing turbulence reports. The region along the trailing edge of jet cirrus (type 4) has a moderately high incidence of turbulence. The least threatening cloud patterns are the anticyclonic leading edge of a baroclinic cloud mass (type 7) and along the southern edge of a rotating low or mid cloud field (type 3).

5. PREVAILING ALTITUDE

For the same five month period described earlier, average altitude and altitude distributions for each of the satellite cloud patterns were determined. For each episode of turbulence, the upper and lower altitude range specified in the pilot reports was used in the computations. The results, summarized in Table 2 show averages between 28,000 and 35,000 ft (8.5-10.5 km) with standard deviations of mostly 5 to 6 thousand ft (1.5-1.8 km). The distribution of altitudes in specified ranges is shown in Figure 14 for each type.

For the purpose of this analysis, type 1 was divided into three segments depending on the location with respect to the satellite-observed upper ridge line, defined as the point of maximum curvature in the cloud band. The segment near the comma head was designated 1a, near the ridge 1b and east of the ridge 1c.

It is significant to note that cloud features which occur near the upper ridge axis (types 1b, 1c, 7 and 8) occur at slightly higher altitudes, on the average. This is due to the higher altitude of the tropopause and jet stream winds at these locations. Features which normally are found near upper troughs or lows (such as 1a, 3 and 6) are located at lower altitudes. In the region of a developing dry slot (type 2) the jet has recently undergone descent (Carlson, 1980) which accounts for the lower average altitudes found there.

Table 2
Average Altitudes of Turbulence Signatures

Signature Type #	Average Altitude (Kft)	σ (Kft)
1a	30.7	5.8
1b	32.2	5.0
1c	31.5	5.6
2	28.1	5.8
3	30.8	5.1
4	31.3	5.1
5	31.3	5.7
6	29.5	5.1
7	33.3	5.1
8	34.5	3.4

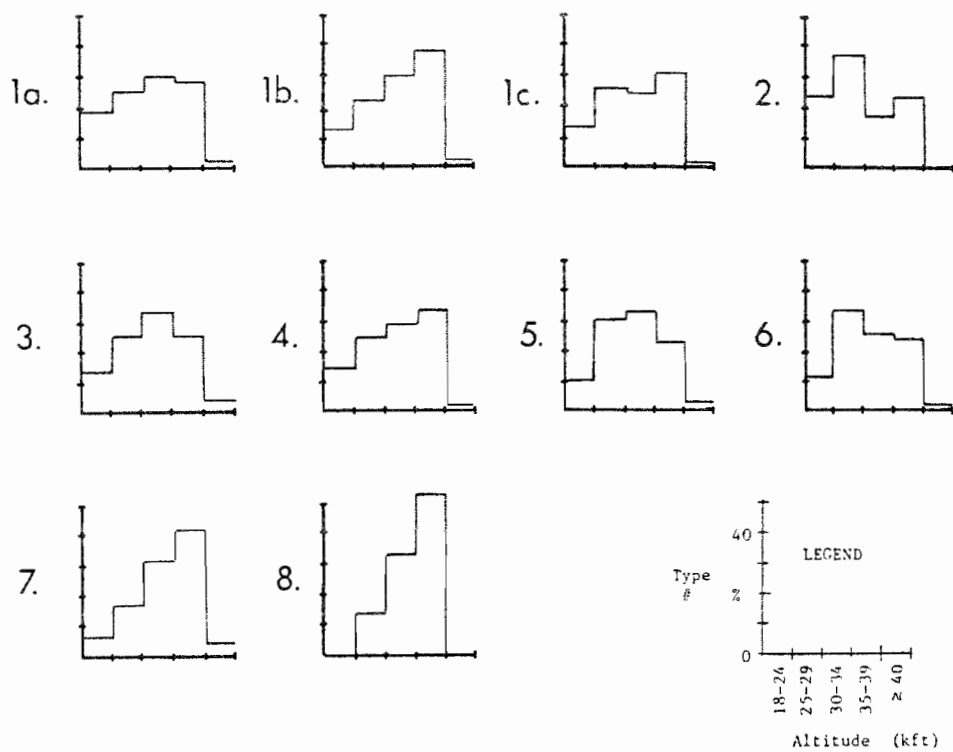


Figure 14 Altitude distribution of turbulence associated with the satellite signatures for a five month period.

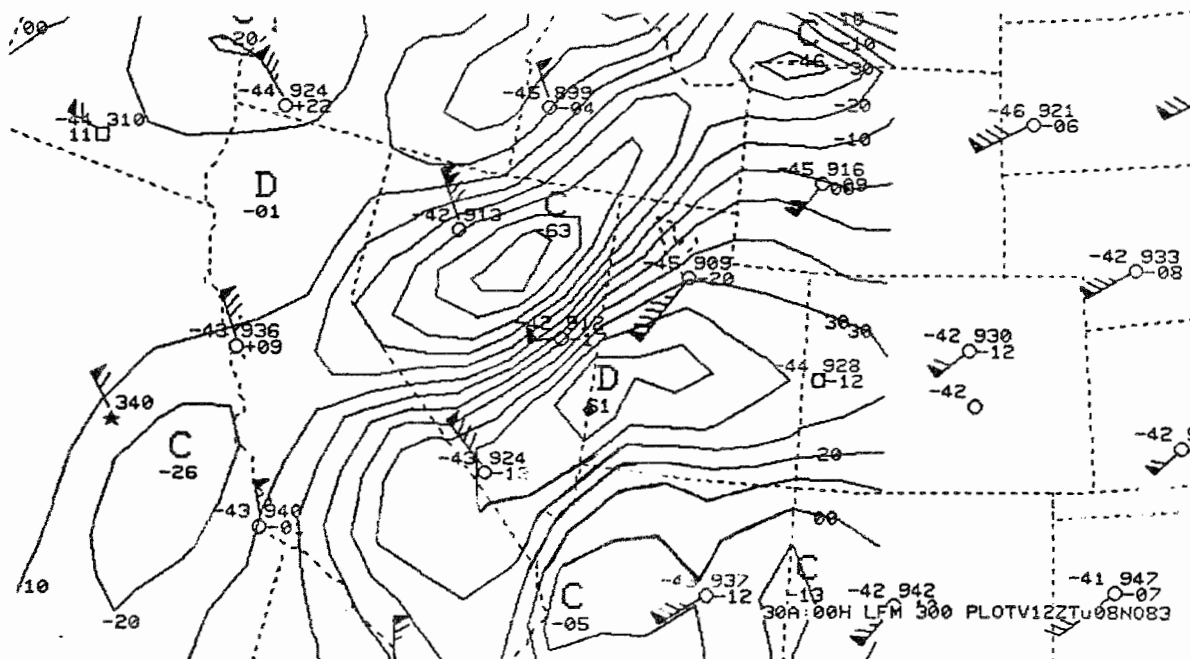


Figure 15 Example of AFOS MES01 divergence analysis. Units are in 10^{-6} sec^{-1} .

6. DISTINGUISHING TURBULENT FROM NON-TURBULENT CLOUD PATTERNS

There are a number of characteristics which may be helpful in distinguishing turbulent from non-turbulent cloud patterns observed in satellite imagery. Most of these can be determined from either the imagery itself or from a combination of imagery and mesoscale analyses derived from conventional upper air data. Two problems exist in using these criteria. First, the 12 hour interval between upper wind reports makes it difficult to detect unforecast changes in the upper level flow. Second, some of these characteristics apply only to certain cloud pattern types and certain special cases within each type. Further studies and refinements will be required to provide more useful guidelines for forecasters. Following are descriptions of distinguishing features found to date.

A. Wind Speed Convergence

(1) Means of Computation

Just a few years ago, the computation of convergence patterns in the atmosphere was considered to be primarily a research tool, beyond the reach of operational weather forecasters. Today, the installation of AFOS (Automation of Field Operations and Services) computer systems at National Weather Service Forecast Offices and McIDAS (Man Computer Interaction Data Access System) at selected central weather facilities provides the capability of obtaining a wide variety of meteorological fields rapidly enough to be of operational use. The McIDAS system is extremely helpful because analyzed data fields can be superimposed directly on the satellite image.

For the purpose of this study, upper-tropospheric convergence or divergence patterns were determined with the MESOL applications program on the Satellite Applications Laboratory's AFOS system. The program obtains radiosonde winds from NMC plot files for standard pressure levels, assigns the u and v components to a grid and then interpolates between grid points. Aircraft and satellite-derived winds are not utilized. The program then determines the divergence:

$$\text{DIV} = \frac{du}{dx} + \frac{dv}{dy} \quad (1)$$

The computed values in units of 10^{-6} sec^{-1} are contoured and assigned to a graphic display. Elements of the program such as grid size, contour interval, pressure level, map background and number of smoothing passes are selectable by the operator (For details on the MESOL program, see Spry and Anderson, 1981). For our purposes, a one degree grid, 10 unit contour interval and two smoothing passes were used. Figure 15 is an example of the output for 300 mb. The program was run for areas of turbulence with detectable cloud signatures for the standard levels nearest the reported altitudes and usually within 3 hours of the reported turbulence. Cases where wind data was missing in key locations were not considered.

(2) Relationship to Turbulence Intensity

For a large number of cases during the fall-winter of 1983-1984, upper level speed divergence was determined in the vicinity of the turbulence cloud feature. In most cases of significant non-convective turbulence, convergence (negative divergence) was observed in the vicinity. Furthermore, the magnitude of turbulence was, in general, directly proportional to the strength of convergence. Figure 16 shows this relationship for areas east of the Rockies and for the region from the Rockies to the west coast. There appears to be no significant difference in the linear best-fit relationship for the two regions although over the Rockies the correlation was weaker. The correlations for both areas were determined to be significant at the 95% level. The large scatter about the lines can be accounted for by a number of factors including: (1) the subjectivity of the turbulence reports (2) the coarse spacing of the upper air reporting network (3) vertical and time variations in the wind field not resolved by standard pressure level data.

A more useful method of displaying this data is shown in the cumulative frequency diagram in Figure 17. Based on this figure, a value of convergence in the range of 40 to $60 \times 10^{-6} \text{ sec}^{-1}$ would most likely produce moderate turbulence. Values in excess of 60 would probably be associated with moderate to severe turbulence. The latter is equivalent to a deceleration of about 50 kt (25 m sec^{-1}) in 4 degree latitude (450 km). The strongest convergence was usually found near the altitudes of reported turbulence.

These results are most useful for large scale cloud systems such as types 1, 3, 4, 7 and 8. The remaining three are smaller in scale and convergence may not be depicted by the existing upper air network. The analyses would be most helpful to forecasters for the early morning forecasts when little information on existing turbulence is available.

The placement of convergence maxima and minima tended to be midway between the upper air stations, thus precise positioning of turbulent regions was usually not possible. However, since maximum convergence often tends to occur near cloud or moisture boundaries, the meteorologist may be able to make subjective adjustments based on the satellite imagery. Poor analyses due to missing winds and sparse or nonexistent data near coastlines were also a problem.

It was noted that some turbulence occurred in regions of upper level divergence. In these cases, the turbulence was normally associated with large, precipitating cloud masses or convection and could not be classified as CAT.

The concept of horizontal convergence as a initiating mechanism for CAT is not new. Kao and Sizoo (1966) found a good correlation between convergence and turbulence in the vicinity of jet streams. Their data were derived from ten research flights east of the Rockies with an instrumented B-47 aircraft. Divergence was computed through the use of radiosondes, pibals and Doppler radar onboard the aircraft. Turbulence was determined with a gust probe plus subjective reports from the pilots. More than 80% of the turbulence occurred with convergent flow including all reports of severe turbulence. The percentage occurrence of severe turbulence increased rapidly as convergence exceeded $100 \times 10^{-6} \text{ sec}^{-1}$. The values in their study are higher than those obtainable from AFOS due to the use of high resolution aircraft Doppler winds.

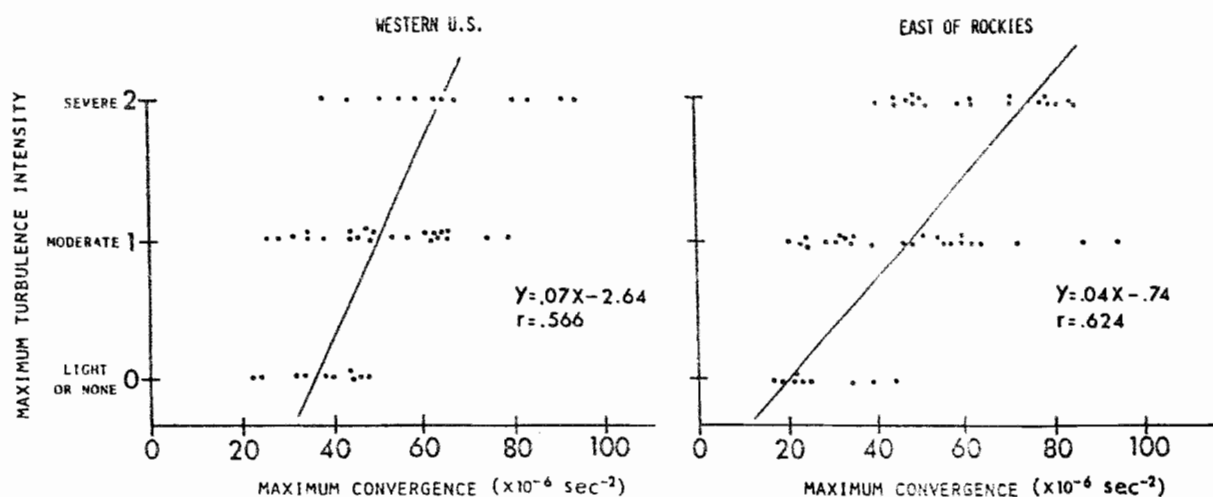


Figure 16 Regression lines showing relationship between maximum convergence determined from MES01 analysis and maximum turbulence intensity for areas over the Rockies (left) and east of the Rockies (right).

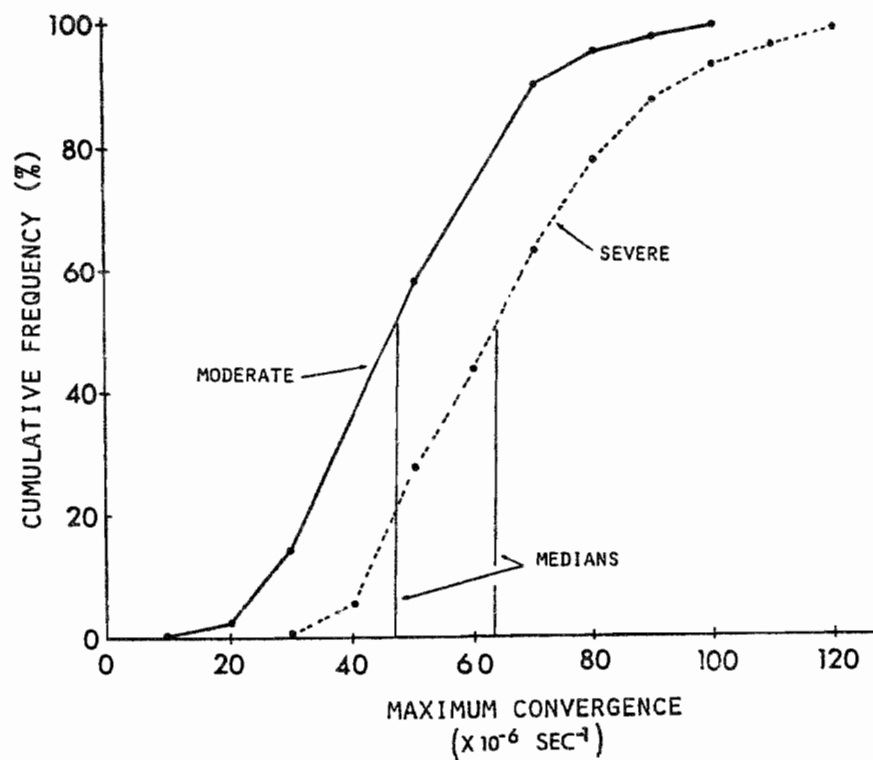


Figure 17 Cumulative frequency (%) for moderate (solid curve) and severe turbulence (dashed) versus maximum convergence.

B. Thermal Gradients

There were a couple of cases of strong convergence which were not accompanied by turbulence. Those situations were differentiated by weak thermal gradients. Strong thermal gradients have been noted to be associated with high probabilities of CAT (Bender and Panofsky, 1976). Operational criteria for significant turbulence include temperature gradients of $>5^{\circ}\text{C}/120\text{ nm}$ oriented across the upper flow (Sorenson and Beckwith, 1975). In one case, turbulence developed within 12 hours as thermal gradients intensified. In general, it has been found that strong convergence with weak thermal gradients produce only light to moderate turbulence. As another example of how thermal gradient information can be used to refine Figure 17, a convergence maximum of $40 \times 10^{-6}\text{ sec}^{-1}$ in the absence of temperature gradients would not likely produce any turbulence.

C. Vorticity Advection Patterns

A simplified form of the vorticity equation for isobaric coordinates is:

$$\underbrace{\mathbf{V} \cdot \nabla (\zeta + f)}_A = - \underbrace{(\zeta + f) \nabla \cdot \mathbf{V}}_B \quad (2)$$

where term A is advection of absolute vorticity and B is divergence. This form of the equation assumes that the local change of vorticity term and the tilting term are both negligible. This assumption is probably valid for the scale of the radiosonde data. The equation states that regions of negative vorticity advection (NVA) (term A is positive) produce high level convergence. Conversely, positive vorticity advection (PVA) results in divergence. From our previous discussion it would follow that most high level non-convective turbulence outbreaks should occur in regions of NVA. Many of the large scale satellite signatures we have described do in fact commonly occur in NVA. This conclusion is based on inspection of upper level vorticity fields and plotted winds produced by the MESOL program on AFOS as well as subjective evaluation of standard level wind charts. Scoggins (1970) also found that NVA is prevalent in turbulent conditions at 300 mb. Turbulence in regions of PVA does occur, but usually in conjunction with convection and not CAT. Instances where NVA is not observed are usually with cloud pattern types 5 and 6 which are often smaller in scale than the radiosonde network. Type 5 may actually be more of a convective type phenomenon.

An example of a case of turbulence accompanied by NVA occurred on April 2, 1984 over the northern plains in association with a major spring storm. The GOES enhanced satellite image at 1500Z (shown earlier in Figure 3) indicated reports of turbulence along the deformation zone north of the major comma cloud system. Figure 18 is the AFOS-produced vorticity and height fields with the wind plots for 250 mb at 00Z on April 3. Strong NVA is occurring over the region of reported turbulence as indicated by strong winds flowing from low toward high values of vorticity.

Unfortunately, except on the McIDAS system, there is no program readily available which quantifies vorticity advection. Until such becomes available, qualitative assessment must continue to be made. Since many forecasters only

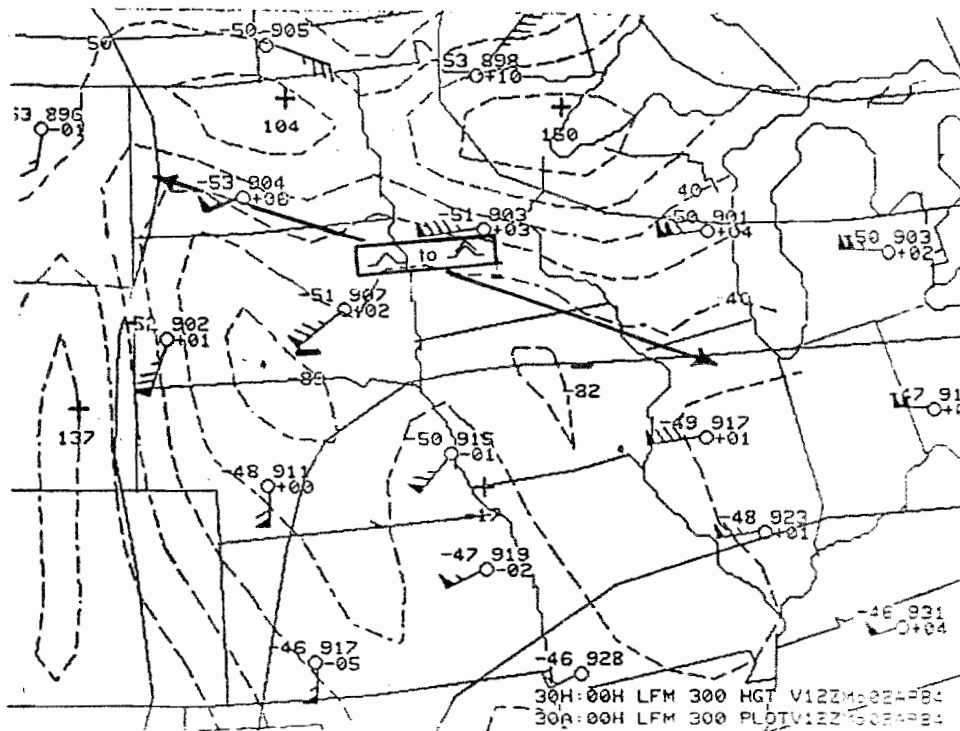


Figure 18 300 mb vorticity and height field with plotted data for 1200Z April 2, 1984, produced by MES01 program.

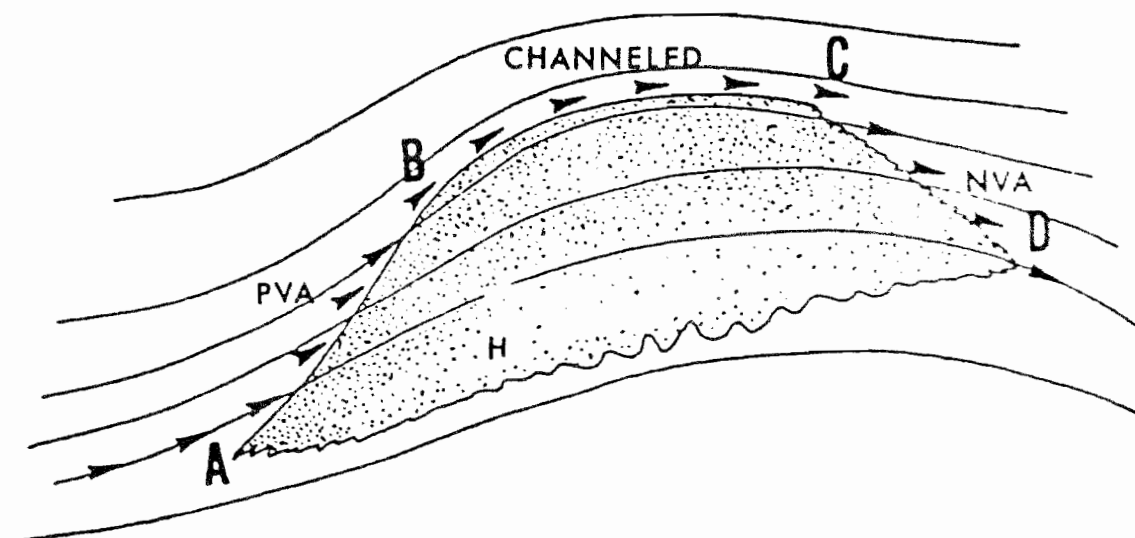


Figure 19 Relationship of jet stream axis to cirrus boundary for NVA, PVA and "channeled" type jet segments (Weldon, 1979).

have access to 500 mb vorticity analyses and forecasts, the question arises as to how vorticity advection patterns at this level compare with those at higher levels. Based on 13 cases examined so far, NVA also occurs at the 500 mb level although, as expected, it is usually much weaker. When the 500mb NVA maximum was displaced with respect to the higher level (which occurred a little less than half the time), it was normally found to the east or south by average of 200-250 nm (370-460 km). This relationship is due to the normal westward slope with height of ridge/trough systems.

It should also be noted from Figures 3 and 18 that the winds tend to cross the cloud boundary at a significant angle. Weldon (1979) describes portions of the jet stream where the isotach maxima are parallel to the cloud boundary but yet whose streamlines cross the cloud edge as "advection" type jets. As the name implies, advection jets relate to areas of NVA and PVA on vorticity charts. Jets which are parallel to cirrus edges and vorticity isoplethes are referred to as "channeled" jets. Figure 19 depicts the relationships just described. Since we have implicated NVA as a prime condition for large scale areas of upper level turbulence, NVA-type jet segments should be strongly suspected as turbulence-producing.

The question may arise as to why turbulence occurs with cloud types 2 and 4 where PVA is normally found. The turbulence could be accounted for by a narrow band of convergence right at the cloud border as suggested by Weldon (1979) and Carlson (1980). Since air within the baroclinic zone cirrus is rising from levels where wind speeds are usually lighter, the intersection of a strong westerly jet with the cloud edge would produce an abrupt decrease in wind speed. Another explanation could be that the turbulence is generated in NVA just west of the upper trough or vorticity lobe in the clear air. Since some time is required for the turbulence to dissipate, it may be experienced east of the trough also.

D. Speeds of Cloud Systems

Most turbulence-producing satellite signatures were found to be fast-moving, usually equal to or greater than 30 knots. An exception is in the vicinity of the head region of comma cloud deformation zones associated with cut off lows. In these cases, turbulence can occur with little movement of the cloud boundary. The rapid approach of an upstream deformation zone or trough is often the key mechanism producing the turbulence in these situations, thus the relative motion with respect to the cloud feature becomes more important. Speeds of satellite-observed cloud systems are routinely contained in Satellite Interpretation Messages (SIMs) produced at the Satellite Field Service Stations (SFSS) and transmitted on both AFOS and standard teletype circuits. Airline forecasters consider a lateral movement of at least 25 kt (12 m sec^{-1}) necessary in order for features near the tropopause to produce turbulence (Sorenson and Beckwith, 1975).

E. Imagery Characteristics

(1) Infrared and Visible

One of the most common (though by no means universal) characteristics of some of the turbulence-producing cloud signatures as observed in the infrared is the sharpness of cloud boundaries. This applies in particular to deformation

zones and the back edge of baroclinic jet cirrus (types 1, 2, 4 and 8). Non-turbulent areas have very diffuse boundaries, often with many thin cirrus lines parallel to the deformation zone or jet cirrus edge which extend over hundreds of kilometers. This is visual evidence of weak convergence and thermal boundaries at upper cloud levels. An example of this in the imagery is shown in Figure 20. When the parallel banding becomes compacted within about 2° to 3° latitude of the main enhanced cloud system, the chances of turbulence increases.

Deformation zones on the north edge of a comma cloud system will sometimes exhibit a pulsating tendency over long periods of time. An initially diffuse cloud boundary will become compact as a jet maximum approaches from the southwest and convergence in the deformation zone increase. When the jet streak turns southeastward over the ridge or dissipates, the cloud boundary may again become poorly defined, and the turbulence threat diminishes. The same cycle may occur along the tail portion of a comma cloud as a jet maximum approaches from the upstream ridge to the northwest. This pulsating tendency has been observed by Weldon (1979) from looking at time-lapse films of satellite photos covering large areas over relatively long time periods (24 hours or more). The strengthening of jet streams was related to a compaction of thermal gradients along the deformation zone caused by an upstream jet.

The foregoing characteristics do not apply at the leading edge of baroclinic zone cirrus east of the upper trough. Here the presence of curved cirrus filaments or transverse spikes is more common in turbulence cases, rather than a sharp, well defined leading edge.

Other supportive indicators previously described are the presence of billow clouds or transverse banding in cirrus clouds or scalloping along the cirrus edge. These indicate a strong likelihood that turbulence is present.

(2) Moisture Channel Imagery

The 6.7 μ m moisture channel from the VAS (VISSR Atmospheric Sounder) instrument onboard the GOES satellites is available operationally at least every six hours. The imagery in this channel represents the integrated radiance emitted by water vapor with a peak response in the middle troposphere near 400 mb. The data has been found to be useful in locating turbulence-producing upper level features such as shortwave troughs, deformation zones, jet streams and vorticity centers which would otherwise be difficult to spot in the 11 μ m window channel infrared (Anderson, et al., 1982). Deformation zones and jet streams, in particular, often appear as sharp boundaries in the moisture channel imagery. Areas of dry air aloft appear darker in the imagery, while high, cold cirrus is white.

Recently, a number of significant turbulent outbreaks have been correlated with a darkening trend with time which appeared in the moisture channel data. The darkening was not related to advection of dry air, but appeared to occur "in situ" as a result of dynamic processes. Turbulence is typically observed within the area of darkening and immediately adjacent to it. The darkening seems to occur simultaneously with reports of turbulence and thus may not always be useful as a precursor. It could be very helpful, however, for the early morning period especially, or at other times when forecasts must be issued without the benefit of recent pireps. When the darkening ceases, turbulence diminishes.

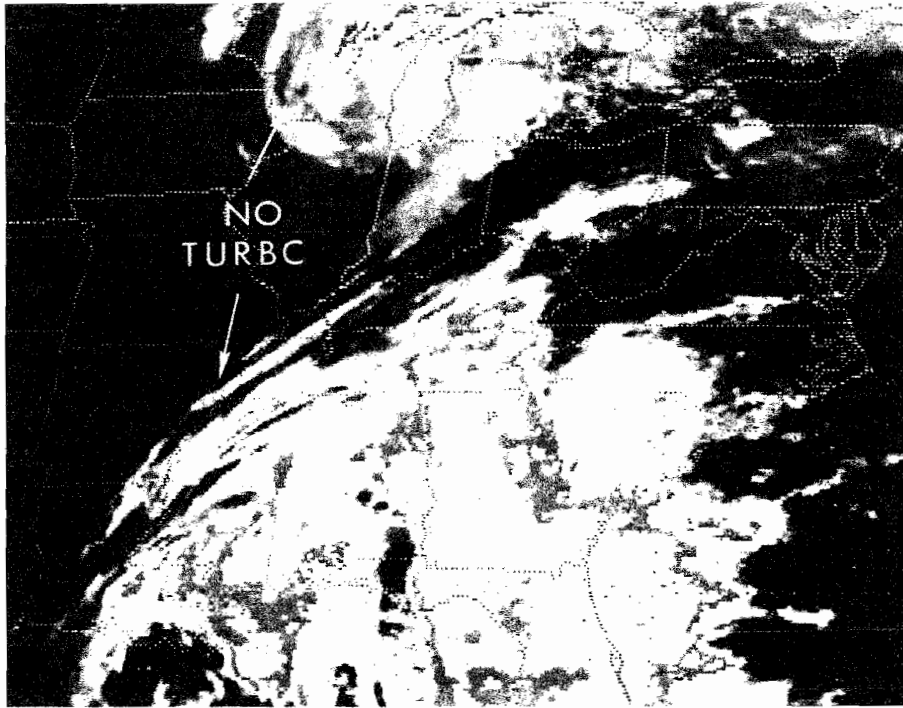


Figure 20 GOES Enhanced IR for February 16, 1983 at 1900Z.

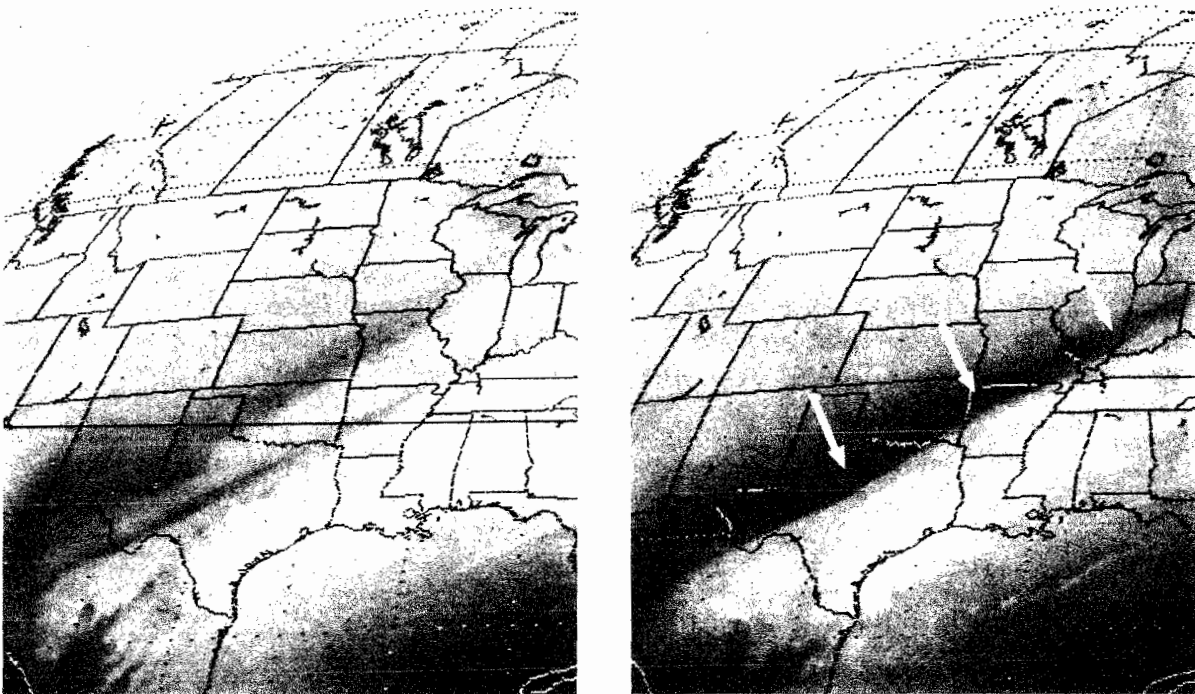


Figure 21 Moisture channel ($6.7\mu\text{m}$) images for 0530Z (left) and 1130Z (right) on January 25, 1984. Arrows show region of pronounced darkening. Turbulence occurred within the dark band and a short distance on either side.

The darkening tends to occur most often in northwest flow type deformation zones, in strong shortwave troughs and near the head region of comma clouds. It has also been observed on the periphery of strong thunderstorms for short periods of time. It is consistent with the findings of strong high level convergence discussed earlier in that mid level subsidence and resultant drying would be expected to occur in these regions. Isentropic cross sections have revealed that the tropopause usually descends or "breaks" during episodes of moisture channel darkening.

Figure 21 is an example of darkening in the moisture channel imagery which occurred on January 25, 1984 from 0530Z to 1130Z. The associated 300 mb flow (Figure 22) shows a northwest flow deformation zone over the central U.S. with a positive tilted (NE-SW) trough. This type of synoptic flow pattern is one of the most common producers of darkening in the water vapor channel. Numerous reports of moderate to severe turbulence occurred during the day (Figure 23) mainly along and to the northwest of the moisture boundary.

During the fall and winter periods of 1983 through 1985 over 100 cases of darkening in the moisture channel imagery were identified. Of these, around 80% had moderate or greater turbulence associated with them while about one third had at least one report of severe turbulence. The altitudes of reported turbulence often sloped from 20 to 30 kft (6.4-9.5 km) along the leading edge of the dark band to 30 to 40 kft (9.5-12.7 km) in the upstream half of the band.

The fact that darkening does not always occur with turbulence episodes is an indication of the complexity of moisture channel interpretation. That is, the observed brightness is related to factors such as; the height, layer thickness, temperature and concentration (mixing ratio) of atmospheric moisture (Weldon and Steinmetz, 1983). Various combinations of these elements can produce the same equivalent brightness on the image. Thus, a darkening which would normally be expected from mid level drying can be counteracted by increases in moisture at lower levels, and/or cold advection. The result would be no noticeable change in brightness. In some instances, a change in brightness occurs but it is too subtle to be observed. The use of new and improved enhancement curves may be a partial solution to the problem.

Variations in photographic density of satellite facsimile machines at field forecast offices are a constant problem and must be considered when comparing consecutive pictures. The use of electronic display devices would make changes in water vapor image brightness much less ambiguous.

Another current difficulty in using moisture channel data is the infrequent availability of images at operational field sites. An interval of 3 hours or less is preferred over the current 6 hours to be operationally useful. Currently, only certain forecast centers and universities which have access to the McIDAS computer system have this capability. More cases must be examined with higher frequency data to determine the utility of the moisture channel for turbulence detection and forecasting.

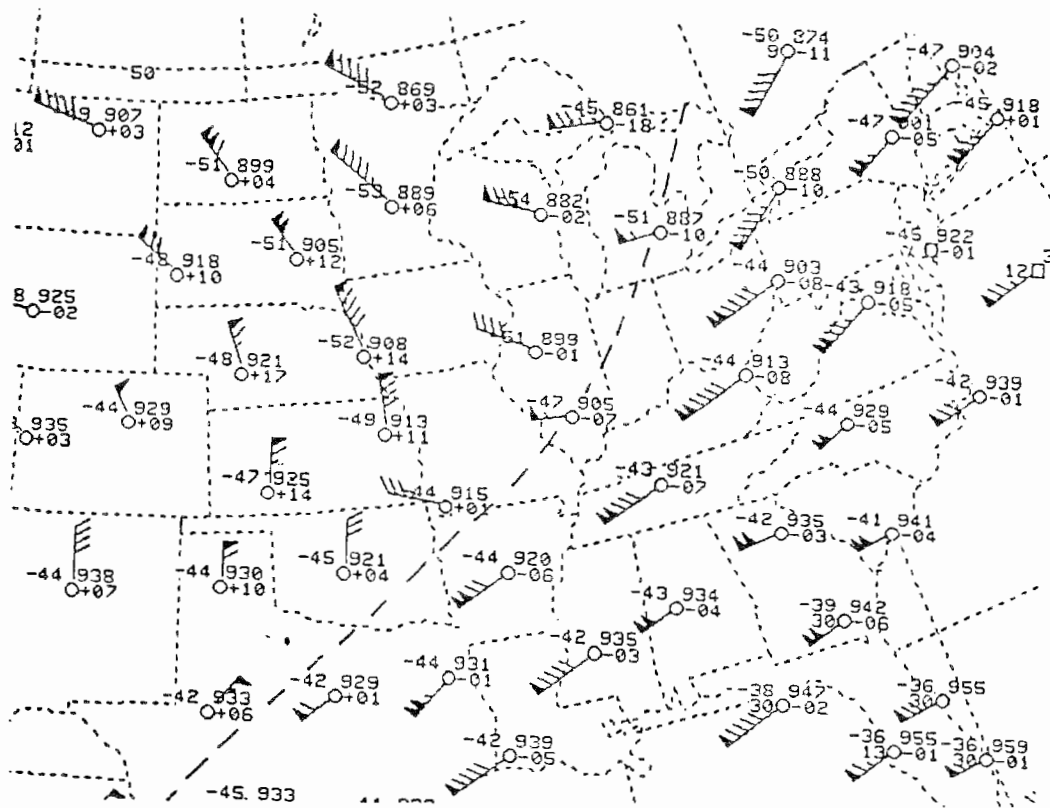


Figure 22 300 mb flow at 1200Z January 25, 1984. Dashed lines show location of upper trough/shear line.

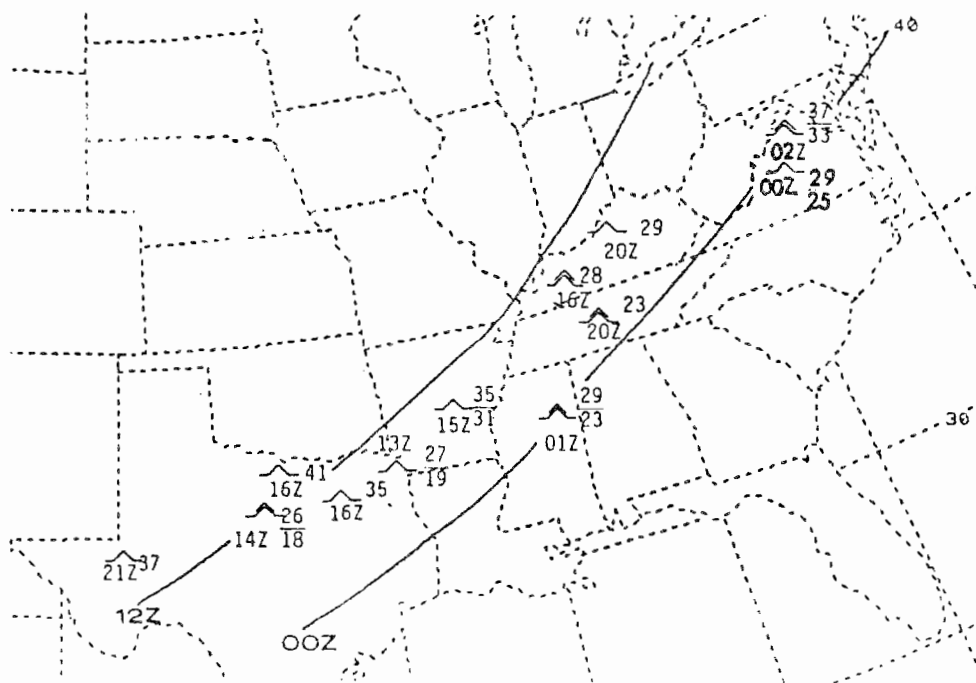


Figure 23 Turbulence observed on January 25-26, 1984 from 1300Z to 0200Z. Solid lines show positions of moisture boundary at 1200Z and 0000Z (estimated at latter time from IR image).

6. CONCLUDING REMARKS

Descriptions of most of the large scale satellite turbulence signatures have been presented along with statistics on their relative frequency and prevailing altitudes. Turbulence occurs most often with cloud features related to deformation zones, jet streaks, ridges and troughs in the upper flow. Strong high level convergence, thermal gradients and in some cases, negative vorticity advection in the region of these cloud patterns appear to be important factors in turbulence production. Direct indications of some of these elements can sometimes be seen in satellite images. Although the accessibility to objectively-produced fields of these parameters has been made much easier by interactive computers, the forecasters must occasionally make subjective adjustments to make the fields relate better to observed cloud or moisture patterns.

It should be emphasized that there are many uncertainties involved in using satellite data alone in turbulence analysis. By judiciously blending satellite and conventional upper air data, however, it seems possible in many cases to locate and track the movement of these turbulent areas and provide useful short range forecasts. Eventually, it may be possible to construct a decision tree to guide the forecaster to a valid decision.

Although the problem of infrequent upper air data remains, the future looks promising in this regard due to the rapid advances in remote sensing technology (Schmidt and Zbar, 1983). Microwave profilers (both land and space-based) may provide frequent vertical wind profiles at many sites by the 1990's. Satellites can now provide dense upper level wind reports based on both cloud displacement vectors and gradients determined from VAS radiance measurements. Upper level winds from commercial jet aircraft (called ASDAR) are now readily available due to rapid transmission to the ground via satellites. These are avenues which should be explored further, since they could provide forecasters with the data they need for more accurate turbulence forecasts.

ACKNOWLEDGEMENTS

The author would like to thank Ralph Anderson and Frank Smigielski of NESDIS and Jim Gurka and Doug Mathews of the NWS for their helpful comments on this report. Jim Kemper and Gerry Rigdon of the NWS provided the AFOS analysis programs used in this study and assisted in their installation. Without the thousands of turbulence reports relayed to the ground by pilots, this study would not have been possible.

REFERENCES

- Anderson, R. K., J. J. Gurka, and S. J. Steinmetz, 1982: Application of VAS Multispectral Imagery to Aviation Forecasting, Preprint Vol., 9th Conf. on Weather Forecasting and Analysis, Seattle, WA, Amer. Meteor. Soc., Boston, 227-234.
- Beckman, S. K., 1981: Wave Clouds and Severe Turbulence, Nat. Wea. Digest, 6, August 1981, 30-37.
- Bender, M. A., and H. Panofsky, 1976: Temperature Gradients and Clear Air Turbulence, Final Report NESS/NOAA Grant No. 04-3-158-60, Penn. State University.
- Carlson, T. N., 1980: Airflow through Midlatitude Cyclones and the Comma Cloud Pattern, Mon. Wea. Rev., 108, 1498-1509.
- Endlich, R. M., 1964: The Mesoscale Structure of Some Regions of Clear Air Turbulence, J. Appl. Meteor., 3, 261-276.
- Gurka, J. J., 1983: Unpublished training notes on CAT detection using satellite data. Satellite Applications Laboratory, NESDIS/NOAA.
- Kao, S. K. and A. H. Sizoo, 1966: Analysis of Clear Air Turbulence Near the Jet Stream, J. of Geophysical Research, 71, 3799-3805.
- Ludlam, R. H., 1967: Characteristics of Billow Clouds and Their Relation to Clear Air Turbulence, Quart. Jour. Royal Met. Soc., 93, 419-435.
- Mancuso, R. L. and Endlich, R. M., 1966: Clear Air Turbulence Frequency as a Function of Wind Shear and Deformation, Mon. Wea. Rev., 94, 581-585.
- Palmén, E. and C. W. Newton, 1969: Atmospheric Circulation Systems, Academic Press, see pages 206-212 and 238-241.
- Rammer, W. A., 1973: Model Relationships of CAT to Upper Wind Flow Patterns, National Meteorological Center Aviation Weather Forecast Branch Note, August 23, 1973, 14 pp.
- Schmidt, H. L. and F. S. Zbar, 1983: NOAA's Long Term Efforts to Improve Weather Forecasting and Service Programs, 5th Symposium on Meteorological Observations and Instrumentation, April 11-15, 1983, Toronto, Canada, 9.1.1-9.1.7.
- Scoggins, J. R., 1970: Meteorological Parameters vs CAT Encountered in Stratosphere by XB-70 Airplanes, Proc. Int. Conference Aerospace and Aeron. Met., May 22-26, 1972, Washington, D.C., 361-366.
- Smigielski, F., 1984: Relating Satellite Observed Cloud Patterns to the Occurrence of High Altitude Turbulence, unpublished Technical Report, Satellite Applications Laboratory, NESDIS/NOAA.
- Sorenson, J.E. and W. B. Beckwith, 1975: Clear Air Turbulence Forecasting as Practiced in Airline Operations, Presented at FAA Symposium of CAT Forecasting, August 12, 1975, Washington, D.C.

- Spry, A.J., and J.L. Anderson, 1981: Mesoscale Objective Analysis, NOAA Western Region Computer Program Series, NWS WRCP - No. 33, Salt Lake City, Utah, 62 pp.
- Viezee, W., R.M. Endlich and S.M. Serebreny, 1967: Satellite-Viewed Jet Stream Clouds in Relation to the Observed Wind Field, J. Appl. Meteor., 6, 929-935.
- Weldon, R., 1979: Cloud Patterns and the Upper Air Wind Field. Part IV, Satellite Training Course Notes, Satellite Applications Laboratory, NESDIS/NOAA, Washington, D.C., 80 pp.